

Article

A Frame Work Design of Chicken-Sine Cosine Algorithm-based Deep Belief Network for Lung Nodule Segmentation and Cancer Detection

G N Beena Bethel ^{1,*}, N Sirisha ², B Kezia Rani ³ and Srikanth Bethu ⁴

¹ Department of CSE, GRIET, Hyderabad, Telangana, India, 1; beenabethel@gmail.com

² Department of CSE, MLRIT, Hyderabad, Telangana, India, 2; nallashirisha@mlrinstitutions.ac.in

³ Department of CSE, VCE, Hyderabad, Telangana, India, 3; keziarani@staff.vce.ac.in

⁴ Department of CSE, GRIET, Hyderabad, Telangana, India, 4; srikanthbethu@gmail.com

* Correspondence: beenabethel@gmail.com

Abstract: Malignant growth is the most widely recognized repulsive infections winning around the world, and the patients with disease are saved just when the malignant growth is distinguished at the beginning phase. Each kind of disease is interesting, with its own arrangement of development properties and hereditary changes. This paper presents the lung knob division and disease characterization by proposing an enhancement calculation. The general technique of the created approach includes four stages, such as pre-processing, division, highlight extraction, and the order. From the outset, the CT picture of the lung is taken care of to the division. When the division is done, the highlights are extricated through morphological and measurable and surface highlights like LOOP and LGP. At long last, the extricated highlights are given to the order step. Here, the characterization is done dependent on the Deep Belief Network (DBN) which is prepared by utilizing the proposed Chicken-Sine Cosine Algorithm (CSCA) which distinguish the lung tumor, giving two classes in particular, knob or non-knob. The presentation assessment of lung knob division and malignant growth grouping dependent on CSCA is figured utilizing three measurements to be specific, precision, affectability, and the explicitness.

Keywords: Chicken-sine Cosine algorithm; Deep Belief Network; Lung nodule detection

1. Introduction

One of the risky ailments brought about by most of the living creatures is disease. Lung malignancy is the sort of disease that starts in lungs. Lungs are considered as the most critical organs in our respiratory framework [11]. It is accounted for by World Health Organization (WHO) [7] that in 2012, this ailment had caused 1.59 million passing's and in 2015, around 158080 passing's happened. The endurance rate relies upon the way that the treatment ought to be begun at beginning phases. It implies on the off chance that it isn't treated at beginning phases; at that point the odds of endurance are less. These days, the death rate is expanded because it is unpredictable for recognizing threatening lung knobs at the previous stage. The estimation of size might be reliable and precise for empowering the evaluation of progress in knob at constrained time span. The time stretch may differ dependent on certain clinical condition. A portion of the lung malignancies, particularly adenocarcinomas are lively than other kind of lung disease, since it might spread the malignant growth cells outside the locale of chest and become dispersed fundamentally, regardless of whether the tumour is extremely little. The size of the knob is multiplied when it estimates 6.3 mm in breadth. On the off chance that the size of the knob is unpredictable, at that point it is intricate for perceiving outwardly. Moreover, the momentary information on the tumor reaction is vital for settling on tolerant explicit treatment choices for better clinical results [4].

Computed Tomography (CT) is the most regularly utilized imaging strategy in thoracic radiology [12]. The lung knob estimations are made with CT for checking the tautomer treatment reason. More up-to-date age-focused on treatments have started to show clinical guarantees in lung disease. Be that as it may, huge numbers of these operators are cytostatic and neglect to influence tumor shrinkage or may surrender the injury shrinkage to the past ages of cytotoxic chemotherapy. The fundamental point of lung tumor location is to identify the lung malignant growth in a previous stage and to lessen the lung disease passing. Consequently, the dangerous decision pathologists don't imply that the patient is an advantage from the treatment of knob. These days, both the picture investigation and picture obtaining approaches permit the semi-robotized tumor division and extraction of a few highlights from pictures. The information from the picture is used for developing prescient and unmistakable models compared to the picture-related highlights to quality protein marks or phenotypes that incorporate clinical information or organic for significant prognostic, analytic, or prescient data. A progressing report demonstrated that early change in tumor volume is more fragile than early estimation changes at EGFR change anticipating in non-little cell lung threatening development. The potential employment volumetric CT may play in dynamically helpful and precise treatment response evaluation is by and by under genuine assessment.

The lung knob division is noteworthy for two unique frameworks like PC helped determination (CAD), and substance-based clinical picture recovery (CBMIR) to forestall or finding of the sores. The underlying CAD framework is used for distinguishing and classifying the knobs as amiable or harmful. The auxiliary CBMIR distinguishes the arrangement of pictures from the database, which have the same qualities as the lung knob. The fundamental point of this framework is to separate the favorable and harmful sores for better analysis [15]. Various classifiers are utilized for characterizing the harmful and benevolent lung knobs, like Artificial Neural Network (ANN) [18], Linear Discriminant Analysis (LDA) [14], and the Support Vector Machine (SVM). Most of the classifiers require information marks for preparing reasons; however, it is over the top expensive for producing named information in radiology. All in all, a portion of the solo calculations are utilized to characterize unlabeled information. Lee et al. [6] created Convolution Neural Networks (CNN) to take in the various leveled portrayals from the unlabeled pictures.

2. Related work

This segment portrays an audit of the writing on different existing lung knob divisions and malignant growth discoveries. These examination papers are taken and assessed by the ongoing distributed years dependent on lung knob division, and malignant growth location strategies

Table 1. Literature review.

Authors	Methods	Advantages	Disadvantages
Palatino linotype	Markov-Gibbs random field (MGRF)	Higher accuracy	Failed to join healthy tissues with the other chest landmarks
Farzad Vasheghani Farahani <i>et al.</i> [8]	Hybrid intelligent Approach	Better segmentation performances	Failed to focus on the feature extraction step to improve the speed and precision
Ganesh Singadkar <i>et al.</i> [9]	The automatic lung segmentation method	Faster and more robust	Failed to develop the segmentation approach while high pathological conditions are available in the lung CT images
Guohui Wei <i>et al.</i> [10]	Local kernel regression models (LKRM)	Achieved a higher classification performance, improved clustering accuracy, and the normalized mutual information	Failed to consider computer-aided categorization approach without segmentation or with segmentation
Qiu Shi <i>et al.</i> [16]	Gestalt-based lung nodule detection Algorithm	Improves performance and computation speed	Contains too many irrelevant units
Shuo Wang <i>et al.</i> [19]	Central Focused CNN (CF-CNN)	Achieved high performance	Two-branch architecture and the Central pooling layer are not considered in the FCN network.
Sudipta Mukhopadhyay [20]	Robust segmentation framework	Improved accuracy	The method completely fails 6 pulmonary nodules from a total 891
Zhiqiong Wang <i>et al.</i> [23]	Semi-supervised extreme learning machine (SS-ELM).	Better performance at a higher learning speed and improved accuracy	The method failed to use unlabeled pulmonary nodules for training

2.1. Challenges to be implemented

- The lung division is testing a result of the in homogeneities in the area of lung, aspiratory structures of same densities, similar to veins, bronchioles, bronchi, conduits, and different examining conventions and scanners.
- Developing exact approval system in the division of lung knob research is exceptionally testing a direct result of manual sore molding utilized by the spectators for planning Ground Truth (GT) divisions is work escalated, making it complex for making colossal GT datasets.
- In Spatial Multi-Kernel FCM, Hybrid clever procedure is created for lung tumor analysis from CT pictures. Here, the presentation was discovered better, yet neglected to analyze 3D preparing rather than 2D for improving the truth of the created technique.
- Lung knob division on the chest CT filters is hard for successful CAD aspiratory infections, similar to lung malignancy. Here, the division precision was discovered better, yet the expense for division id high [3].

- The significant test for lung knob division is merge rules. However, the shape imperative is thought of, unpredictable molded knobs stay critical for preparing in light of the fact that shape theory is disregarded.

An ordered record of the inception of malignant growth registers and uncommon studies to determine disease occurrence, with subtleties of the data requested in each occasion, is introduced. Comparisons made between rates obtained for lung cancer in 12 regions where it is to be accepted that 90% or a higher amount of all malignancies happening has been recorded. The standard interims between the beginning of first side effects and enlistment at death for diseases of various locales considered, and the extents of cases recorded upon death endorsements just, and it is recommended that exactness old enough explicit rates might be improved by utilizing the age at the beginning of first indications as a basis rather than age at registration or death, and that "inception rates" so derived are more meaningful.

3. Materials and Methods

The essential objective of this exploration is to structure and present a methodology for lung knob division and malignant growth identification by proposing a streamlining calculation. The general method of the proposed approach includes four stages, pre-preparing, lung knob division, highlight extraction, and grouping. At first, the CT lung picture will be exposed to the pre-handling. After pre-handling, the lung knob division will be completed dependent on adjusted Spatial Multi-Kernel FCM [2] in which a few piece capacities, such as Gaussian, exponential, and digressive will be used. After the division of lung knobs, the element extraction will be performed dependent on Morphological and factual highlights, like elasticity, entropy, roundness, differentiate, homogeneity, circularity, vitality, connection, standard deviation, mean, territory, Euler number, significant pivot length, direction, robustness, and the surface highlights, like LOOP and Local Gradient Pattern (LGP) [21]. At long last, the order will be done dependent on the extricated highlights utilizing Deep Belief Network (DBN) that are prepared to utilize the proposed Chicken-Sine Cosine Algorithm (CSCA). The proposed CSCA is planned by joining Chicken Swarm Optimization [13], and Sine Cosine Algorithm for lung tumor identification, giving two classes, which incorporate non-knob, and knob. The square chart of the lung tumor division and malignant growth identification approach utilizing the proposed CSCA appears in figure 1The Materials and Methods should be described with sufficient details to allow others to replicate and build on the published results. Please note that the publication of your manuscript implicates that you must make all materials, data, computer code, and protocols associated with the publication available to readers. Please disclose at the submission stage any restrictions on the availability of materials or information. New methods and protocols should be described in detail while well-established methods can be briefly described and appropriately cited.

Adenocarcinoma in situ (AIS) is a pre-intrusive injury in the lung and a subtype of lung adenocarcinoma. The patients with AIS can be quieted by dismissing the injury. Inquisitively, patients with noticeable lung adenocarcinoma have a shocking 5-year duration rate. AIS can outline noticeable lung adenocarcinoma. The evaluation and relationship of AIS and noticeable lung adenocarcinoma at the genomic level can extend our comprehension of the instrument's crucial lung perilous advancement improvement.

As of now, I saw 61 lung adenocarcinomas (LUAD) noticeable express differentially passed-on attributes, including nine long non-coding RNAs (lncRNAs) given RNA sequencing procedures (RNA-seq) information from standard, AIS, and interfering tissue tests. These qualities showed concordant Differential Enunciation (DE) structures in the free stage III LUAD tissues acquired from The Cancer Genome Atlas (TCGA). For individual conspicuous unequivocal attributes, we amassed sub frameworks utilizing the Genetic Algorithm (GA) given protein-protein composed endeavors, protein-DNA affiliations, and lncRNA rules. Our evaluation perceived an aggregate of 19 center sub sorts out that included intrusive express attributes and, in any case, one putative lung risk driver

quality. Convenient appraisal of the center sub frameworks uncovered their improvement in known pathways and regular advances in danger for tumor headway and attack, including the VEGF hailing pathway and the negative principle of cell progression.

Lung nodule segmentation

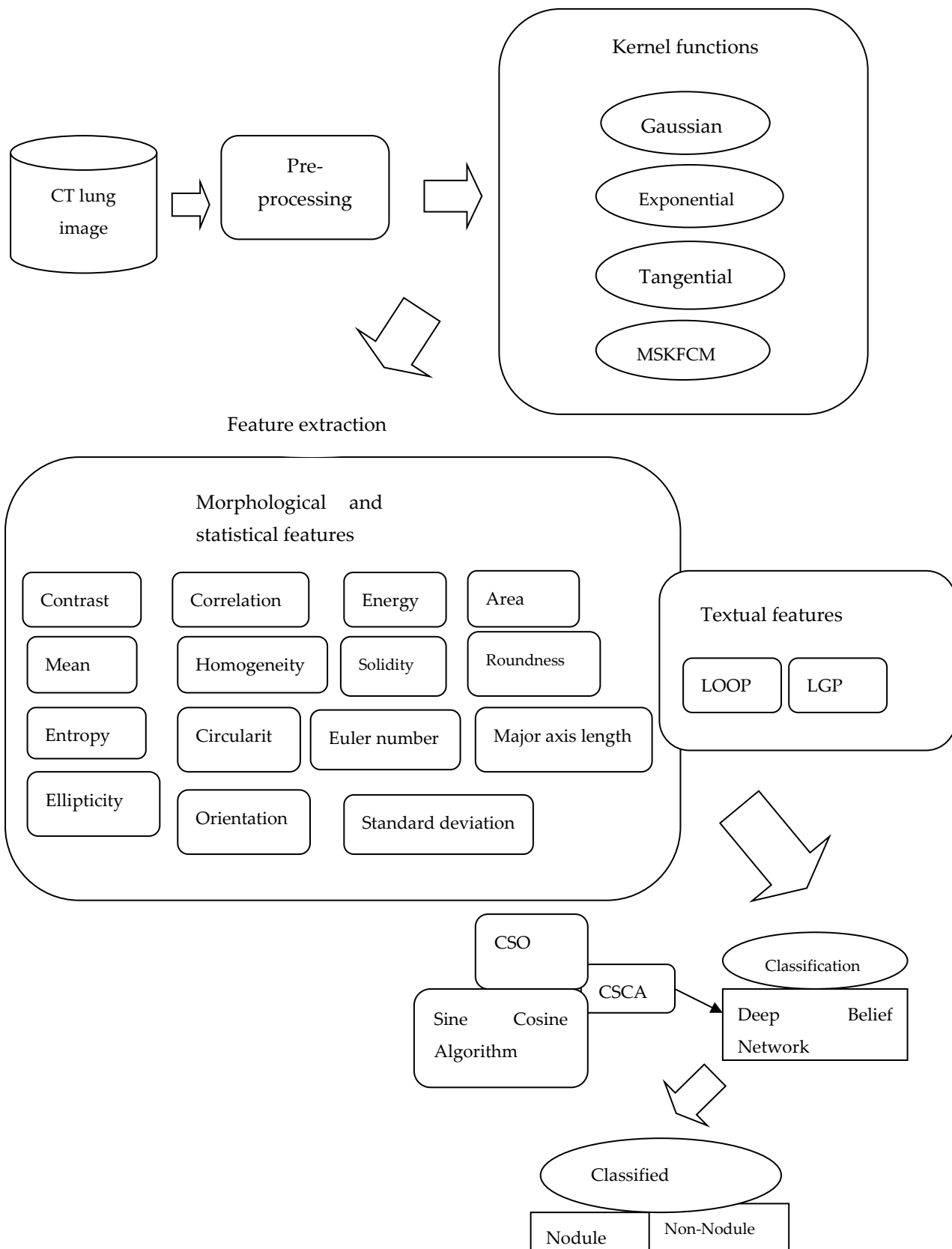


Figure 1. Frame -work design of Lung nodule segmentation.

Computed Tomography (CT) is the most ordinarily utilized imaging system in thoracic radiology. The lung knob estimations are made with CT for observing the tumor treatment reasons. More current age focused on treatments have started to show clinical guaranteesng malignancy. Huge numbers of these specialists are cytostatic and neglected to influence tumor shrinkage or may abandon the injury shrinkage than the past ages of cytotoxic chemotherapy. The fundamental point of lung tumor mortification is to distinguish the lung malignancy in a prior stage and to decrease the lung disease passing.

Consequently, the threat decision by the pathologists does not imply that the patient is an advantage from the treatment of knob. These days, both the picture investigation and picture obtaining approaches permit the semi-mechanized tumor division and extraction of a few highlights from pictures. The information from the picture is used for developing prescient and enlightening models comparing to the picture related highlights to quality protein marks or phenotypes that incorporate clinical information or natural for important prognostic, symptomatic, or the prescient data. An advancing report indicated that new change in tumor volume is touchier than the early partition across change at EGFR change, imagining in non-little cell lung hurtful turn of events. The potential occupation volumetric CT may play in progressively supportive and definite treatment reaction evaluation is beginning at now under concentrated appraisal.

The lung knob division is vast for two unique frameworks like PC supported finding (CAD), and substance-based clinical picture recovery (CBMIR) to forestall or determination of the sores. The underlying CAD framework is used for recognizing and ordering the knobs as considerate or threatening. The optional CBMIR recognizes the arrangement of pictures from the database, which have the same attributes as the lung knob. The primary point of this framework is to separate the benevolent and dangerous sores for better analysis. Various classifiers are utilized for grouping the dangerous and considerate lung knobs, like ANN, LDA, and SVM. A large portion of the classifiers requires information names for preparing reason. However, it is pricey for creating named information in radiology. When all is said in done, a portion of the unaided calculations is utilized to arrange unlabeled information.

3.1. Implementation

From the earliest starting point, the proposed approach uses a sort II soft figuring to improve harsh CT pictures. By that point, a novel division calculation subject to cushy c-infers bunching, called Modified Spatial Kernelized Fuzzy c-infers (MSFCM) gathering, is offered so as to accomplish another delineation of lung regions through a movement approach. Next, handle applicants are perceived among every single accessible thing in the lung zones by a morphological system. This is followed by evacuating fundamental genuine and morphological highlights from such handle, all in all, an outfit of three classifiers containing Multilayer Perceptron (MLP), KNN, and SVM is utilized for the real finding and picking if the handle candidate is handle (harm) or non-handle (prosperity).

Considerably more essentially, extraordinary obliging execution estimations in clinical applications including precision, affectability, unequivocally, turmoil arrange, likewise as the space under the Receiver Operating Characteristic (ROC) contort are figured. The got outcomes to admit the promising demonstration of the proposed mixture procedure in got a handle on aspiratory handles finding.

From figure 1, the Artificial Intelligence application model is planned to utilize Machine Learning calculations for a forecast of results. The accompanying stages are utilized to execute this calculation. In the first stage information is procured from Wisconsin lung malignant growth database and pre-prepared utilizing the managed calculations as demonstrated figure 2.

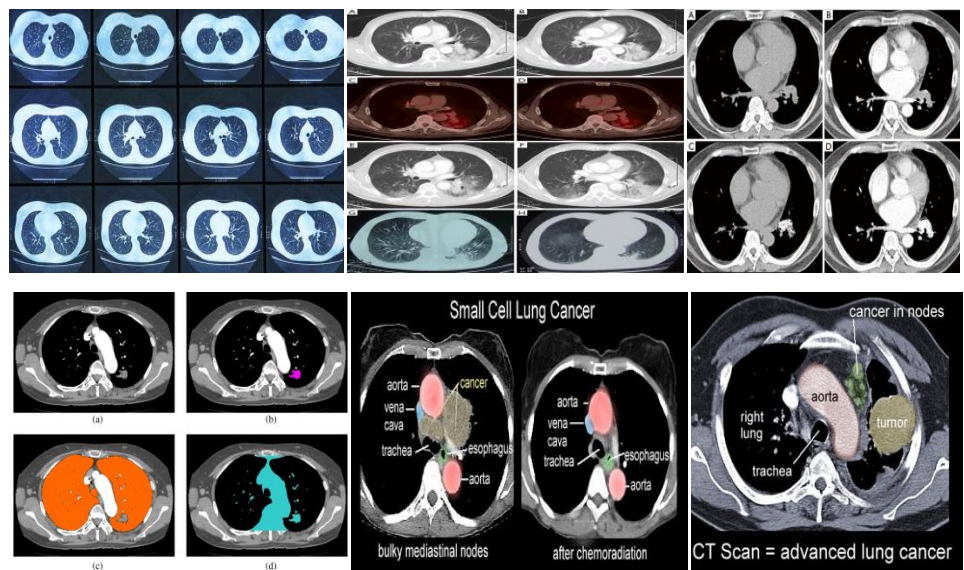


Figure 2. Lung nodule images pre-processing sample dataset.

In Figure 2, a sample dataset of CT lung images is processed and checked the presence of cancer nodes. In this paper, we have utilized more than 1000 images for the classification of lung nodules. The images are taken from all the aged people both mammals females. We have noticed every image carefully to identify for which age it was occurring and, we noticed the cause for this happening. Here lung nodule is taken as one of the feature extraction attribute to classify these images. Using the above images dataset, we have prepared a table to process the dataset into a system for better segmentation to predict better results in feature. We have indicated pulmonary areas with colors in above images for a better view.

Table 2. Patients' parameters to create dataset.

Gender	Male and Female
Age group	16-25, 26-35, 36-50, 51-65, 66-75, 75+
Physical condition	Disabled or not disabled
Mental health condition	Good or bad
Long-standing illness	Yes or no
Employment status	Full time, Part time, Student, Retired, Home maker, Retired seeking to job
Clinical information characteristics	Aorta, Vena, Trachia, Cava, Tumor, Esophagus, Lung, Skin, Sarcoma, Prostate
Patient status	In-patient and Day-case
Ethnicity	White, Black, Mixed
Time first admitted	<1 year, 1-2 years, <5 years, >5 years
Responding to treatment	Yes, No, Responded after joining

From the above Table 2, we have arranged our gathered data from all over the world (using Wisconsin dataset and kaggle dataset), using the patient characteristics. These characteristics are used to design pre-processing data and converted into .csv file to process into AI system model.

3.1.1. Lung Nodule Segmentation – Mathematical Functions

In Second phase lung nodule segmentation, kernel functions are used to separate the labelled and unlabeled data using feature extraction and feature selection methods

like Gaussian, exponential, tangential and Modified Spatial Kernelized Fuzzy C-Means (MSKFCM). This kernel reduces the dimensionality between the dataset attributes and produces the only defined variables. The defined variables are calculated using attribute bias and variance values. The purpose of finding these values is to know how the designed model is producing the accuracy. So all the processed dataset variables are arranged in form of matrix and avoiding the unwanted elements to reduce the cost function and search space.

The Gaussian part (assortment of irregular factors ordered by time or space) is characterized in 1-D, 2D and N-D individually as, for discretionary genuine constants a , b and non zero c . The boundary is the stature of the bend's pinnacle, b is the situation of the focal point of the pinnacle and c controls the width of the "ringer". From Figure 3, Gaussian capacities are frequently used to speak to the likelihood thickness capacity of an ordinarily disseminated irregular variable with expected worth $\mu = b$ and fluctuation $\sigma^2 = c^2$. For this situation, the Gaussian is of the structure given in eq. (1)

$$f(x) = ae^{-\frac{(x-b)^2}{2c^2}} \quad \text{and} \quad g(x) = \frac{1}{\sigma\sqrt{2\pi}}e^{-\frac{1}{2}(\frac{x-y}{\sigma})^2} \quad (\text{eq. 1})$$

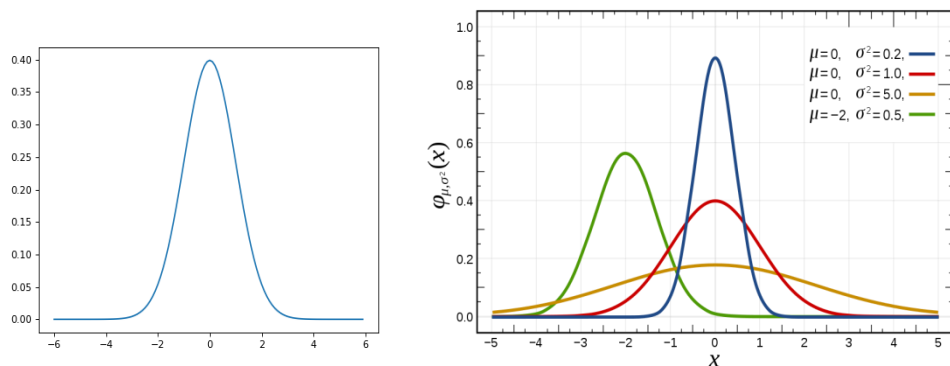


Figure 3. Gaussian form with expected value μ and variance σ^2 , $b = \mu, c = \sigma$.

The Exponential kernel function covariance function is defined by eq. (2).

$$k(x_i, x_j | \theta) = \sigma^2 f \exp\left(-\frac{r}{\sigma_1}\right) \text{ where } \sigma_1 \text{ is the characteristic length scale and}$$

$$r = \sqrt{(x_i - x_j)^T (x_i - x_j)} \text{ is the Euclidean distance } x_i \text{ and } x_j \quad \text{eq. (2)}$$

In the investigation of ANNs, the Neural Tangential Kernel (NTK) is a portion which portrays the development of profound counterfeit neural systems during their preparation by inclination plunge. It permits ANNs to be contemplated utilizing hypothetical instruments from Kernel Methods. For most normal neural system structures, in the constraint of huge layer width the NTK gets consistent. This empowers straightforward shut structure articulations to be made about neural system forecasts, preparing elements, speculation, and misfortune surfaces. For instance, it ensures that enormous enough ANNs unite to a worldwide least when prepared to limit an observational misfortune. The NTK of enormous width systems is likewise identified with a few other huge widths cut off points of neural systems and the equation given as eq. (3).

Let's bring in some notation:

- Call the neural network function $f(x, x)f(w, w)$ where xx the input is and ww is the combined vector of weights (say of size pp).
- In this 1-D example, our dataset will just be points $(x, y), (x, Y)$. Let's say we have NN of them, then dataset is: $\{x_i, y_i\}N_i = \{x_i, y_i\} = 1N$.

For learning the network, we'll take a simple approach again: just perform full-batch gradient descent on the least squares loss. Now, you might be familiar with writing this loss as

$$L(w) = \frac{1}{N} \sum_{i=1}^N \frac{1}{2} (f(\bar{x}_i, w) - \bar{y}_i)^2 \quad \text{eq. (3)}$$

But we can simplify this using some vector notation.

First, stack all the output dataset values y_i, \bar{y}_i into a single vector of size NN , and call it y, \bar{y} .

Similarly, stack all the model outputs for each input, $f(x_i, w), f(w, x_i)$ into a single prediction vector $y(x) \in RN, y(w) \in RN$.

We basically have $y(w)i = f(x_i, w)y(w)i = f(x_i, w)$. This is similar in flavor to looking at the neural network function $f(\cdot, w)f(\cdot, w)$ as a single vector belonging to a function space.

So, our loss simplifies to this: $L(w) = \frac{1}{N} \frac{1}{2} \|y(w) - \bar{y}\|_2^2$

Now, from Figure 4, we won't be changing the dataset size NN anywhere, and it's an unnecessary constant in the loss expression. So, we can just drop it without affecting any of the further results, while making the algebra look less cluttered $L(w) = \frac{1}{2} \|y(w) - \bar{y}\|_2^2$

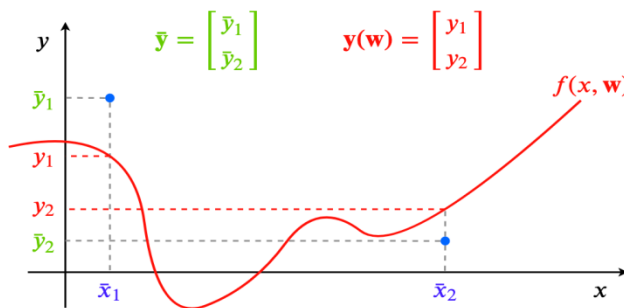


Figure 4. Vector notation representation.

From the figure 5, If the weights double, this relative change will be 2 irrespective of the size of the hidden layers. Now if we plot this for the nets we trained above:

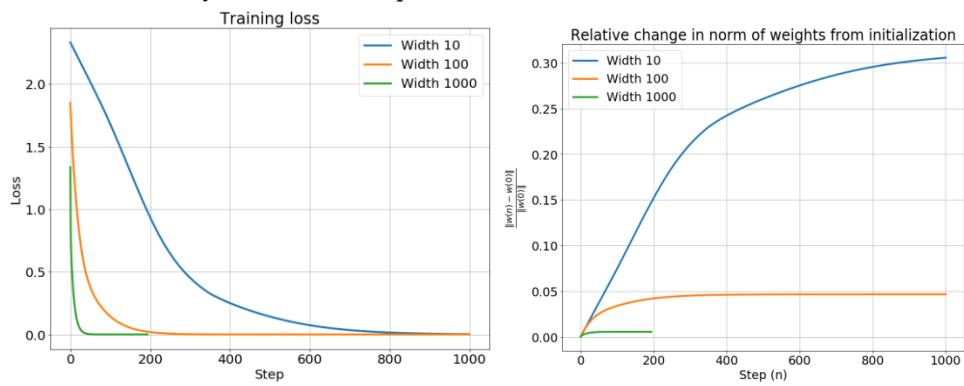


Figure 5. Training Loss and Relative change in weights.

Fuzzy Clustering (moreover insinuated as fragile gathering or sensitive k-suggests) each data point can have a spot with more than one gathering. Gathering or bundle assessment incorporates consigning data centres to packs with the ultimate objective that things in a comparative gathering are as equivalent as could sensibly be normal, while things having a spot with different gatherings are as dissimilar as could sensibly be normal. Gatherings are recognized by methods for closeness measures. These likeness

estimates join division, accessibility, and force. Particular likeness measures may be picked reliant on the data or the application.

In non-fuzzy clustering (in any case called hard gathering), data is detached into specific packs, where each data point can simply have a spot with correctly one gathering. In cushioned gathering, data centres can possibly have a spot with various bundles. For example, an apple can be red or green (hard packing), yet an apple can moreover be red AND green (cushy gathering). Here, the apple can be red with a particular goal in mind similarly as green with a particular goal in mind. Instead of the apple having a spot with green [green = 1] and not red [red = 0], the apple can have a spot with green [green = 0.5] and red [red = 0.5]. These values are normalized some place in the scope of 0 and 1; regardless, they don't address probabilities, so the two characteristics don't need to mean 1.

The mostly used Fuzzy Clustering Algorithm is the Fuzzy C-Means Clustering Algorithm. The fuzzy c-means algorithm is in a general sense equivalent to the k-means algorithm:

- Choose different bundles.
- Assign coefficients self-assertively to each data point for being in the packs.
- Repeat until the estimation has joined together (that is, the coefficients' change between two emphases is near ϵ , the given affectability limit)
- Compute the centroid for each bundle (exhibited as follows).
- Every data point, figure coefficients of presence in their gatherings.

The point x coefficients degree of presence in the k th pack is $w_k(x)$. The centroid gathering is the mean equivalent is weighted by the degree of having a spot with the pack, or, numerically, addressed in eq. (4).

$$C_k = \frac{\sum_x W_x(x)^m x}{\sum_x W_x(x)^m} \quad \text{eq. (4)}$$

here m is termed as hyper-boundary. The calculation endeavours to segment a limited assortment of n components $X = \{X_1, \dots, X_n\}$ into an assortment of c fluffy bunches as for some given basis. Given a limited arrangement of information, the calculation restores a rundown of c bunch focuses $C = \{C_1, \dots, C_c\}$ and a segment framework style. The FCM minimized objective function from eq. (5).

$$\arg \min_c \sum_{i=1}^n \sum_{j=1}^c W_{ij}^m \|x_i - C_j\|^2 \quad \text{where } W_{ij} = \frac{1}{\sum_{k=1}^c \left(\frac{\|x_i - C_k\|}{\|x_i - C_k\|} \right)^{\frac{2}{m-1}}} \quad \text{eq. (5)}$$

3.1.2. Feature Extraction

Contrast, Mean, Entropy, Elasticity, Correlation, Homogeneity, Circularity, Orientation, Energy, Solidity, Euler number, Standard deviation, Area, Roundness, Major axis length are taken as a Morphological features and Statistics in image processing. Loop and LGP are taken as Textual Features in this paper.

3.1.3. Chicken – Sine Cosine Algorithm

It is exceptionally basic from the scientific and algorithmic points of view. It gives in numerous cases exceptionally exact outcomes. This calculation probably won't have the option to beat after calculations on explicit arrangement of issues. Presences of four arbitrary boundaries are accessible. In this paper, the Tent guide is applied to a close by interest reliant on the best individual of the chicken huge number, and the subjectively picked chicken is superseded by the picked individual. Scattered chicken huge number smoothing out is proposed finally. The key centers are delineated as follows.

3.1.4. Adaptation Search and Probability

This interest is progressively convincing in a little space; anyway it requires a long exertion to glance in an enormous space, which impacts the capability of the estimation. In this paper, search space is adaptively adjusted by the progression of the estimation.

$$X_{min}(d) = \text{best } X(d) - |\text{best } X(d)| * \alpha \quad \text{eq. (6a)}$$

$$X_{max}(d) = \text{best } X(d) + |\text{best } X(d)| * \alpha \quad \text{(eq. (6b)}$$

Where $X_{min}(d)$ lower bound of search is space for d_{th} dimension and $X_{max}(d)$ is upper bound for search space for d_{th} dimension, $\text{best } X(d)$ is d_{th} dimension of individuals and $\alpha \in (0, 0.5)$ is search factor. The decrease value in convergence rate probability is adjusted to $P_t = 1 - \frac{1}{1 + \log t}$ eq. (6c)

Algorithm 1. Chicken Algorithm.

Chicken Algorithm

Stage 1: Determine the boundaries size N, no. of cycles M, singular measurements d, refreshed recurrence G, the no of chickens, hens, chicks and mother hens P1, P2, P3 and P4 following coefficients FL, Cmax is most extreme disorderly inquiry α is search factor.

Stage 2: Initialize the chick esteem that is arbitrarily produced between the upper and lower limits and do emphases.

Stage 3: Update swarm esteems

Stage 4: Select best fit worth

Stage 5: Randomly select a chicken esteem and supplant with best fit worth.

Stage 6: If the most extreme no of emphases arrived at then stop, if not bring 3 back.

The Sine Cosine Algorithm (SCA) is a populace based meta-heuristic calculation in which it utilized the sine and cosine capacities to look for the ideal arrangement. In this manner, the SCA calculations, like other MH calculations, begins by producing a lot of N arrangements called X utilizing the accompanying condition.

A nonlinear programming problem is stated as follows

$$\text{Min}_{\cap} f(x) = f(x_1, x_2, \dots, x_n) \in R^n \text{ subject to: } x \in \cap$$

$$\cap = \left\{ x \mid g_j(x) \leq 0, j = 1, \dots, q, h_j(x) = 0, j = q + 1, \dots, m \right. \\ \left. < B_i \leq x_i \leq U B_i, i = 1, \dots, n \right\} \quad \text{eq. (6d)}$$

Global minimum: for the function $f: \cap \subseteq i^n \rightarrow R, \cap \neq \emptyset$, the value $f^1 @ f(x^1)$ is called a global minimum if and only if $\forall x \in \cap: f(x^*) \leq f(x)$.

$$X_i = l_i + r \text{ and } X(\mu_i - l_i), i = 1, \dots, N$$

$$X_i^{t+1} = \left\{ \begin{array}{l} X_i^t + r_1 * \sin(r_2) * |r_3 P_i^t - X_i^t|, r_4 < 0.5 \\ X_i^t + r_1 * \cos(r_2) * |r_3 P_i^t - X_i^t|, r_4 \geq 0.5 \end{array} \right\} \quad \text{eq. (6e)}$$

$$r_1 = a - \frac{a * T}{T} \text{ and } r_2 = a - t \frac{a}{\max} \quad \text{eq. (6f)}$$

Algorithm 2. Sine-Cosine Algorithm.**Sine-Cosine Algorithm**

Stage 1: Initialise the area for search specialists

Stage 2: Evaluate the inquiry specialist by target work

Stage 3: Update the area of the acquired best arrangement

Stage 4: Update the boundaries r1, r2, r3 and r4

Stage 5: Update the situation of search operators

Stage 6: Record the best arrangement

Where r1 shows next bit locales, r2 characterizes how for the development ought to be towards or outwards, r3 gives irregular loads for goal so as to stochastically underscore ($r3>1$) or deemphasize ($r3<1$) the impact of desalination in characterizing the separation. At long last the boundary r4 similarly switches between the sine and cosine segments.

3.1.5. Deep Belief Networks (DBN)

Deep Belief Networks are utilized to perceive, group and create pictures, video successions and movement catch information. A ceaseless profound conviction arranges is just an augmentation of a profound conviction organized that acknowledges a continuum of decimals, instead of paired information. DBN model joint distribution between observed vector x and l hidden layers h^k as follows

The below equation is a conditional distribution for the visible conditioned units on the hidden units of the RBM (Restricted Boltzman Machines) at each level k and $P(h^{k-1}|h^k)$ is the visible-hidden joint distribution in the top-level.

Boltzmann Machines (BMs) are a particular kind of log-straight Markov Random Field (MRF), i.e., for which the essentialness work is immediate in its free limits. To make them inconceivable enough to address snared movements (i.e., go from the compelled parametric setting to a non-parametric one), we consider that a portion of the elements are infrequently watched (they are rung secured). By having continuously covered variables (furthermore called disguised units), we can grow the showing furthest reaches of the Boltzmann Machine (BM). Constrained Boltzmann Machines further restrict BMs to those without observable clear and concealed covered affiliations. The vitality capacity of RBM is given in eq. (7a) and loads W associating shrouded layer and noticeable layer units and b, c are given as free vitality recipe in eq. (7b).

$$P(x, h^1, \dots, h^l) = (\prod_{k=0}^{l-2} P(h^k | h^{k+1})) P(h^{l-1}, h^l) \text{ where } x = h^0, P(h^{k-1}|h^k) \text{ eq(7)}$$

$$E(v, h) \text{ and } E(v, h) = -b'v - c' - h'Wv \quad \text{eq. (7a)}$$

$$F(v) = -b'v - \sum_i \log \sum_{h_i} e^{h_i(c_i + w_i v)} \quad \text{eq(7b).}$$

4. Results

The resulted outcome of the proposed Chicken-Sine Cosine Algorithm (CSCA) will be greater than the accuracy of 96.5%, sensitivity of 93.2%, and the specificity of 98.1%, which have been obtained by the method modified Spatial Kernelized fuzzy c-means (MSFCM) and ensemble learning. The implementation of the proposed approach done in MATLAB and the dataset that employed is LIDC-IDRI [22]. The performance of the proposed technique for lung tumor [5] segmentation, and cancer detection evaluated using three metrics, namely accuracy, sensitivity and specificity, and the results attained compared with that of existing works

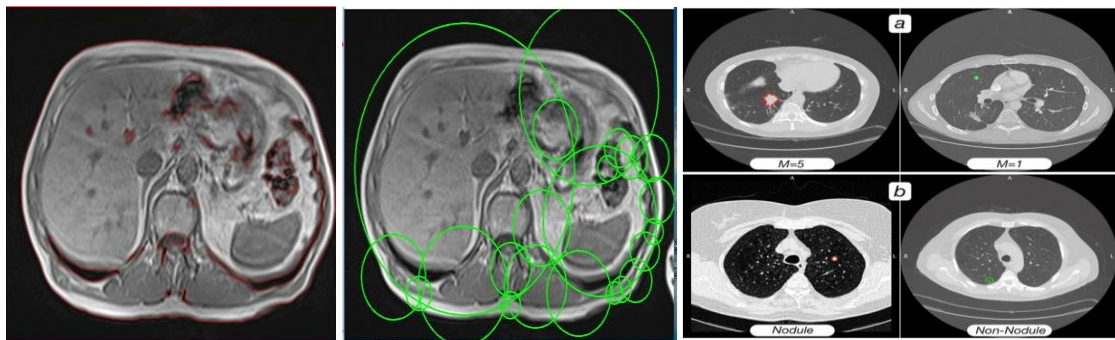


Figure 6. The result of Nodule Segmentation produced from trained dataset is divided into individual segmented images and classified as nodule and non-nodule images by keeping CT slice thickness M=5(nodule) and M=1 (non-nodule).

Table 3. Sensitivity calculation values.

Solid Modules	Slice thickness (mm)	Lung nodule segmentation values				Deep Belief Network P value
		Chicken Sine Cosine values	Xmin	Xmax	Pt	
>=5	26	5	9.6	84.4	72	0.91
>=6	14	5	10.4	89.4	78	0.92
>=7	10	5	12.8	90.6	86	0.93
>=8	5	5	14.0	88.5	75	0.89
>=5	26	1	3.3	50.3	44	0.94
>=6	14	1	5.13.1	55.7	48	0.95
>=7	10	1	3.4	52.4	49	0.96
>=8	5	1	3.2	51.3	48	0.97

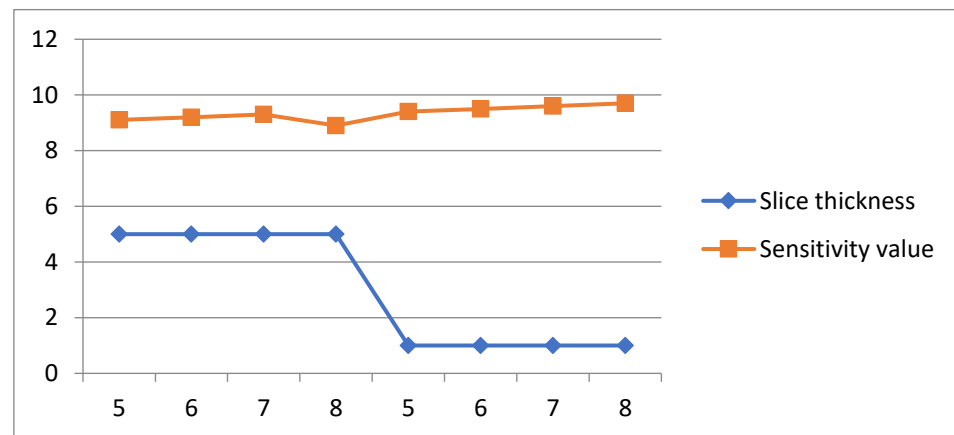
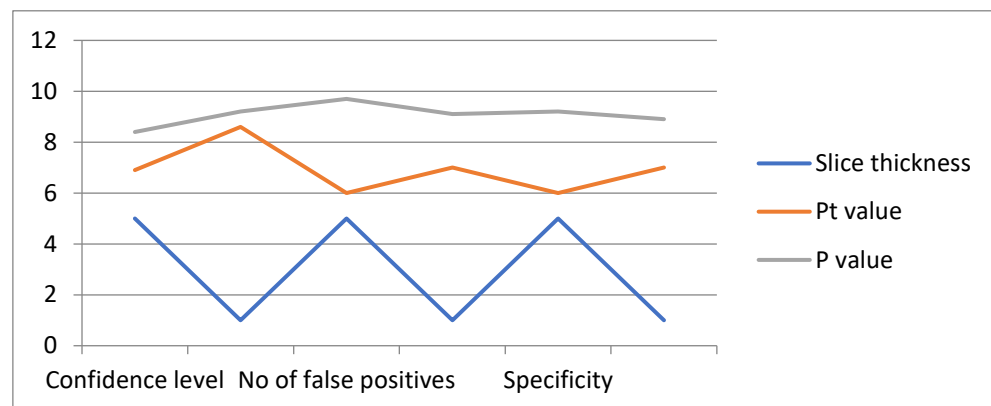


Figure 7. Sensitivity representation Graph.

Table 4. Specificity calculation values.

Parameter	Slice thickness (mm)	Lung nodule segmentation values			
		Chicken Sine Cosine values	Xmin	Xmax	Deep Belief Network P value
Confidence Level %	5	9.7	9.7	69	0.84
	1	10.0	10.2	86	0.92
No of false positives	5	65.3	53.5	120.2	0.97
	1	46.1	186.4	268.1	0.91
Specificity	5	22.5	29.9	59.1	0.92
	1	27.5	35.1	70.2	0.89

**Figure 8.** Specificity representation graph.

In the figure 6, it is shown Nodule and Non-Nodule segmented images. Here the thickness of CT slice is M=5 and M=1. The below Table 3 and Table 4 gives information of calculations of Sine Cosine algorithm and Deep Belief Network values irrespective of Sensitivity, Specificity and Figure 7 and Figure 8 represents the their graph.

$$Accuracy = \frac{P_{\max \text{ method value}} - P_{\max \text{ reference value}}}{P_{\max \text{ reference value}}}$$

Table 5. Performance comparison of Datasets used in nodule segmentation process.

Performance comparison of Dataset used for nodule segmentation process				
Dataset type	Method	Sensitivity %	Specificity %	Accuracy %
LIDC-IDRI	Tumor Net	83.20	87.20	89.50
	DFC Net	86.20	84.50	88.40
	Cmix Net	94.50	90.20	90.30
Hospital Data	Tumor Net	82.50	8.010	82.20
	DFC Net	84.67	77.12	78.44
	Cmix Net	88.00	84.45	84.70

Table 6. Performance comparison of algorithms.

Algorithm name	Sensitivity %	Specificity %	Accuracy %
Chicken Sine Cosine	99	92	91
CNN	97	84	90
Boltzmann Machine	96	88	89
ANN	98	90	90
RNN	95	80	90

The above Table 5 gives the performance comparison of datasets used in this paper. Table 6 gives information of performance of algorithms.

5. Conclusions

Nodule depends on the Deep Belief Network (DBN) highlight articulation just as the radiological quantitative picture includes articulation. For foreseeing harmful lung knobs utilizing CT filter pictures, we utilized totally isolated datasets for preparing and for approval. We led a precise report and examination of the models. The Figure 6, 7 and 8 are produced when dataset is arranged according Table 2, 3 and 4 characteristics. The algorithms are compared with same dataset and results are given in Table 5 and 6.

The profound learning-based knob order results were additionally assessed with various elements, for example, tolerant family ancestry, age, smoking history, clinical biomarkers, size, and area of the distinguished knob. A ton of investigations were performed on the publically accessible LIDC-IDRI datasets. The agreement danger rating was the normal of all harm appraisals appointed to all cuts remembered for the last accord division, adjusted to the closest whole number. "Non-knob" areas were sectioned utilizing a mechanized Python programming library. Te sectioned areas were additionally prepared by a MATLAB library to create the quantitative picture highlights estimations. The exhibition assessment of lung knob division and malignant growth arrangement dependent on CSCA is registered utilizing three measurements correctly, exactness, affectability, and the particularity. Results show the predominance of the proposed framework with lesser computational expense. Finally we conclude that the combination of Chicken Swarm and Sine Cosine Algorithms producing the high accurate results when compared with other optimization techniques. The same proposed method can also applicable in finding the Breast Cancer, Heart Disease etc.

Acknowledgments: In this section, Thanks to R&D Departments of GRIET College , Telangana, Hyderabad, India. Thanks to Government of Telangana for providing data.

Conflicts of Interest: No conflicts of interest

References

1. Ahmed Soliman, Fahmi Khalifa, Ahmed Elnakib, Mohamed Abou, El-Ghar, Neal Dunlap, Brian Wang, Georgy Gimel'farb, Robert Keynton, and Ayman El-Baz, " Accurate Lungs Segmentation on CT Chest Images by Adaptive Appearance-Guided Shape Modeling", IEEE Transaction on Medical Imaging, Vol:36,no:1,pp:263-276,January 2017
2. Amer G. Binsaadoon and El-Sayed M. El-Alfy,"Gait-based Recognition for Human Identification using Fuzzy Local Binary Patterns", In ICAART, vol.2, pp. 314-321, 2016.
3. Ananya Bhattacharjee and Swanirbhar Majumder," Automated Computer-Aided Lung Cancer Detection System", Advances in Communication, Devices and Networking, pp. 425-433, February 2019.
4. Ayman El-Baz, Garth M. Beach, Georgy Gimel'farb, Kenji Suzuki, Kazunori Okada, Ahmed Elnakib, Ahmed Soliman, and Behnoush Abdollahi, "Computer-Aided Diagnosis Systems for Lung Cancer: Challenges and Methodologies", Hindawi Publishing Corporation International Journal of Biomedical Imaging, pp.46, November 2012.
5. B. Zhao, L. H. Schwartz, C. Moskowitz, M. S. Ginsberg, N. A. Rizvi, and M. G. Kris, "Computerized quantification of tumor response in lung cancer: Initial results," Radiology vol.241, pp. 892-898, 2006.
6. By Honglak Lee, Roger Grosse, Rajesh Ranganath and Andrew Y. Ng, " Unsupervised Learning of Hierarchical Representations with Convolutional Deep Belief Networks", Communications of the ACM, vol. 54, no.10, pp.95-103, October 2011.

7. David Forman, Jacques Ferlay, Bernard W. Stewart, and Christopher P. Wild, "World Cancer Report 2014", International Agency for Research on Cancer, World Health Organization, Lyon, 2014.
8. Farzad Vasheghani Farahani, Abbas Ahmadi, Mohammad Hossein Fazel Zarandi, "Hybrid intelligent approach for diagnosis of the lung nodule from CT images using spatial kernelized fuzzy c-means and ensemble learning", Mathematics and Computers in Simulation vol. 149, pp. 48-68, July 2018.
9. Ganesh Singadkar, Abhishek Mahajan, Meenakshi Thakur and Sanjay Talbar, " Automatic Lung Segmentation for the Inclusion of Juxtaleural Nodules and Pulmonary Vessels using Curvature based Border Correction", Journal of King Saud University - Computer and Information Sciences, July 2018.
10. Guohui Wei, He Ma, Wei Qian, Fangfang Han, Hongyang Jiang, Shouliang Qi and Min Qiu, " Lung nodule classification using local kernel regression models with out-of-sample extension", Biomedical Signal Processing and Control, vol.40, pp.1-9, February 2018.
11. Highly accurate model for prediction of lung nodule malignancy with CT scans by Jason L. Causey.
12. I. Sluimer, A. Schilham, M. Prokop, and B. van Ginneken, " Computer analysis of computed tomography scans of the lung: a survey", IEEE Transactions on Medical Imaging, vol. 25, no. 4, pp. 385 – 405, April 2006.
13. Improved Chicken Swarm Algorithms Based on Chaos Theory and Its Application in Wind Power Interval Prediction by Bing Wang.
14. Meng X, Liu Y, Gao X and Zhang H , "A New Bio-inspired Algorithm: Chicken Swarm Optimization," Advances in Swarm Intelligence, 86–94, 2014.
15. Priyanshu Tripathia, Shweta Tyagia, and Madhwendra Nath, "A Comparative Analysis of Segmentation Techniques for Lung Cancer Detection1", Pattern Recognition and Image Analysis, vol. 29, no. 1, pp. 167–173, January 2019.
16. Qiu Shi, Wen Desheng, Cui Ying and Feng Jun, " Lung Nodules Detection in CT Images Using Gestalt-Based Algorithm", Chinese Journal of Electronics, Vol:25, no:4, July 2016.
17. S. Mirjalili, "SCA: A Sine Cosine Algorithm for solving optimization problems," Knowledge-Based Systems, vol. 96, pp. 120–133, 2016.
18. Seyedali Mirjalili, "SCA: A Sine Cosine Algorithm for Solving Optimization Problems", Knowledge-Based Systems, vol. 96, no.15, pp. 120-133, March 2016.
19. Shuo Wang, Mu Zhou, Zaiyi Liu, Zhenyu Liu, Dongsheng Gu, Yali Zang, Di Dong, Olivier Gevaert and Jie Tiana, " Central Focused Convolutional Neural Networks: Developing a Data-driven Model for Lung Nodule Segmentation", Medical Image Analysis, Vol:40, pp:172-183, August 2017.
20. Sudipta Mukhopadhyay, " A Segmentation Framework of Pulmonary Nodules in Lung CT Images", Journal of Medical Imaging, Vol:29, no:1, pp:86-103, February 2016.
21. Tapabrata Chakraborti, Brendan McCane, Steven Mills and Umapada Pal, "LOOP Descriptor: Encoding Repeated Local Patterns for Fine-grained Visual Identification of Lepidoptera", October 2015.
22. The Cancer Imaging Archive (TCIA) Public Access, taken from "<https://wiki.cancerimagingarchive.net/display/Public/LIDC-IDRI>", accessed on September 2018.
23. Zhiqiong Wang, Junchang Xin, Peishun Sun, Zhixiang Lin, Yudong Yao and Xiaosong Gao, " Improved Lung Nodule Diagnosis Accuracy Using Lung CT Images With Uncertain Class", Computer Methods and Programs in Biomedicine, Vol:162, pp: 197-209, August 2018.